nature COMMUNICATIONS

ARTICLE

DOI: 10.1038/s41467-017-02754-z OPEN

Early Cambrian fuxianhuiids from China reveal origin of the gnathobasic protopodite in euarthropods

Jie Yang[1], Javier Ortega-Hernández[2,3], David A. Legg[4], Tian Lan[5], Jin-bo Hou[1] & Xi-guang Zhang[1]

Euarthropods owe their evolutionary and ecological success to the morphological plasticity of their appendages. Although this variability is partly expressed in the specialization of the protopodite for a feeding function in the post-deutocerebral limbs, the origin of the former structure among Cambrian representatives remains uncertain. Here, we describe *Alacaris mirabilis* gen. et sp. nov. from the early Cambrian Xiaoshiba Lagerstätte in China, which reveals the proximal organization of fuxianhuiid appendages in exceptional detail. Proximally, the post-deutocerebral limbs possess an antero-posteriorly compressed protopodite with robust spines. The protopodite is attached to an endopod with more than a dozen podomeres, and an oval flap-shaped exopod. The gnathal edges of the protopodites form an axial food groove along the ventral side of the body, indicating a predatory/scavenging autecology. A cladistic analysis indicates that the fuxianhuiid protopodite represents the phylogenetically earliest occurrence of substantial proximal differentiation within stem-group Euarthropoda illuminating the origin of gnathobasic feeding.

[1] Key Laboratory for Palaeobiology, Yunnan University, Kunming 650091, China. [2] Department of Zoology, University of Cambridge, Downing Street, Cambridge CB2 3EJ, UK. [3] Department of Organismic and Evolutionary Biology and Museum of Comparative Zoology, Harvard University, 26 Oxford Street, Cambridge, MA 02138, USA. [4] Department of Earth, Atmospheric, and Environmental Sciences, University of Manchester, Manchester M13 9PL, UK. [5] College of Resources and Environmental Engineering, Guizhou University, Guiyang 550003, China. Correspondence and requests for materials should be addressed to X.-g.Z. (email: xgzhang@ynu.edu.cn)

Euarthropod appendages are characterized by the selective proximodistal (PD) differentiation of specific podomeres for various purposes, including locomotion, feeding, and sensing[1–4]. Despite its significance for the ecological success of these organisms, the early evolution of PD limb differentiation in the Cambrian stem lineage has only received minimal scrutiny. The origin of the protopodite—the specialized basal part of the post-deutocerebral limbs in crown-group euarthropods—is of critical importance in this context given its involvement in gnathobasic feeding[1,5–9]. Current hypotheses postulate that the appendicular organization of the crown-group evolved by the fusion of the proximal podomeres in the biramous limbs of Cambrian taxa, resulting in the simultaneous origin of the protopodite and the seven-segmented endopod observed in several representatives[5,10,11]. The fuxianhuiids—a group of stem-group euarthropods exclusively known from the Cambrian of South China—occupy a central role in these hypotheses, as their appendages have been regarded as an evolutionary link between the lobopods of soft-bodied ancestors[12] and the arthropodized limbs of Deuteropoda (i.e., upper stem-group Euarthropoda + crown-group Euarthropoda)[13]. Problematically, the basal portion of the fuxianhuiid post-deutocerebral appendages remains completely unknown despite numerous studies on the anatomy of these fossil organisms[14–19].

Here we describe the proximal functional morphology of post-deutocerebral appendages in three fuxianhuiid species based on exceptionally preserved fossil specimens from the early Cambrian (Stage 3) Xiaoshiba Lagerstätte in South China[12,14]. Our material includes a new taxon and provides direct evidence for the early evolution of the specialized protopodite with a feeding function within the euarthropod stem lineage.

Results

Systematic palaeontology.

(Upper stem-group) Euarthropoda Lankester 1904 (see discussion in ref. [13])

Fuxianhuiida Bousfield 1995

Chengjiangocarididae Hou and Bergström 1997

Constituent taxa. *Chengjiangocaris longiformis* Hou and Bergström, 1991[15] (Cambrian Stage 3, Chengjiang); *Chengjiangocaris kunmingensis* Yang et al., 2013[14] (Cambrian Stage 3, Xiaoshiba); *Alacaris mirabilis* gen. et sp. nov. (Cambrian Stage 3, Xiaoshiba). See also Supplementary Note 1.

Alacaris mirabilis gen. et sp. nov.

Etymology. After *Ala*, a village about 3.7 km northwest of the Xiaoshiba section; *caris* (Latin), shrimp; *mirab* (Latin), miracle, referring to the unexpected discovery of gnathal structures in fuxianhuiids limbs.

Type material. Yunnan Key Laboratory for Palaeobiology, Yunnan University; YKLP 12268 (holotype), a complete individual preserved in lateroventral view, showing details of the articulated appendages (Fig. 1a). YKLP 12269 (paratype), an articulated individual preserved in lateral view showing the complete organization of the dorsal exoskeleton and the ventral limbs (Fig. 1f).

Other material. 37 topotype specimens, YKLP 12270–12306.

Locality and horizon. Xiaoshiba section in Kunming, South China (Cambrian Series 2, Stage 3; local lower Canglangpuan Stage); lower portion of the Hongjingshao Formation typified by the presence of trilobite *Zhangshania*, corresponding to the *Yilangella–Zhangshania* biozone[20], approximately 10 m above the *Yunnanocephalus–Chengjiangaspis–Hongshiyanaspis* trilobite biozone[12] (Supplementary Fig. 1).

Diagnosis. Fuxianhuiid with heart-shaped head shield associated with eye-bearing anterior sclerite. Body composed of 13 overlapping tergites with pleurae that narrow posteriorly, plus a conical tailspine with lateral flukes. Five anteriormost tergites greatly reduced relative to the rest of the trunk, covered by head shield in life position. Appendages consist of elongate (deutocerebral) antennae, followed by a set of (tritocerebral) specialized post-antennal appendages (SPAs), and several pairs of biramous limbs. Four pairs of post-antennal limbs bear a robust protopodite with gnathobasic endites. Endopods consist of more than a dozen podomeres (i.e., multipodomerous), and a prominent terminal claw. Exopod flap like. Mouth opening and proximal bases of SPAs concealed by a broad hypostome with anterior margin extension, defined by lateral slits.

Remarks. *Alacaris* is similar to *Chengjiangocaris* in general body architecture, most notably the possession of a heart-shaped head shield, a broad butterfly-shaped hypostome, five anteriormost reduced trunk tergites, and other trunk tergites that taper in width posteriorly without expanded pleurae[14–17]. *Alacaris* differs from *Chengjiangocaris* in the presence of only 13 trunk tergites, the more robust construction of the SPAs with serrated edges, and less developed lateral wing-like extensions on the hypostome.

Description. Individuals reach 12 cm in maximum length. The dorsal exoskeletal morphology consists of a sub-elliptical anterior sclerite connected to a pair of lateral stalked eyes (Fig. 1g, h and Supplementary Fig. 2c–e). The anterior sclerite articulates with a broad heart-shaped head shield that covers the cephalic region and part of the trunk. The head shield is frequently taphonomically displaced[14], revealing details of the underlying anatomy (Fig. 1a, f, g and Supplementary Figs 2a, c and 3). The trunk comprises 13 tergites (T*n*) with a sub-rectangular outline (Fig. 1a, f and Supplementary Fig. 4c). T1 to T5 are greatly reduced, and together reach a sagittal length similar to T6 (Supplementary Figs 2a, f and 4a, c, d); these tergites are covered by the head shield in life position. T1 to T5 widen progressively posteriorly, and have anteriorly reflexed pleura with rounded margins. T6 to T13 maintain a sub-equal length throughout the body, but taper in width posteriorly (Fig. 1 and Supplementary Figs 2, 4); the pleurae have rounded anterior margins, and acute posterior ones. The tailspine has a conical shape, and is associated with a pair of tail flukes with posterior-facing setae (Fig. 1a and Supplementary Fig. 4c, e).

The ventral organization of the head includes a pair of deutocerebral[14,21] pre-oral antennae composed of approximately 20 articles that narrow distally (Fig. 1b, g, h and Supplementary Fig. 2c, d, g, h). The antennae attach close to the anterior margin of the hypostome, the sclerotized plate that covers the mouth (Fig. 1a–c, g, h and Supplementary Figs 2c, d and 3a, b). The hypostome has a broadly subtrapezoidal outline. The anterior margin extends medially, and is delimited by a pair of short slit-like lateral furrows. The lateral margins form wing-like extensions with straight edges. The posterior margin has a medial notch that conveys a bilobed appearance. The following limbs are a pair of tritocerebral[14,22] SPAs that occupy a para-oral position (Fig. 1a–c and Supplementary Fig. 2a, b, h, j), and whose proximal halves are covered by the hypostome. The SPAs consist of three robust sub-rectangular podomeres (P*n*). P1 is the shortest, and is distinguished by the presence of short spinose endites that form a medially oriented gnathal edge (Fig. 1b, c, and Supplementary Fig. 3a, b). P2 is the longest, and articulates with P3, which bears an acute distal termination and a strong spine on its posterior blade-like margin (Supplementary Fig. 2h–j). The surface of the SPAs is covered by coarse tubercles, which together with their

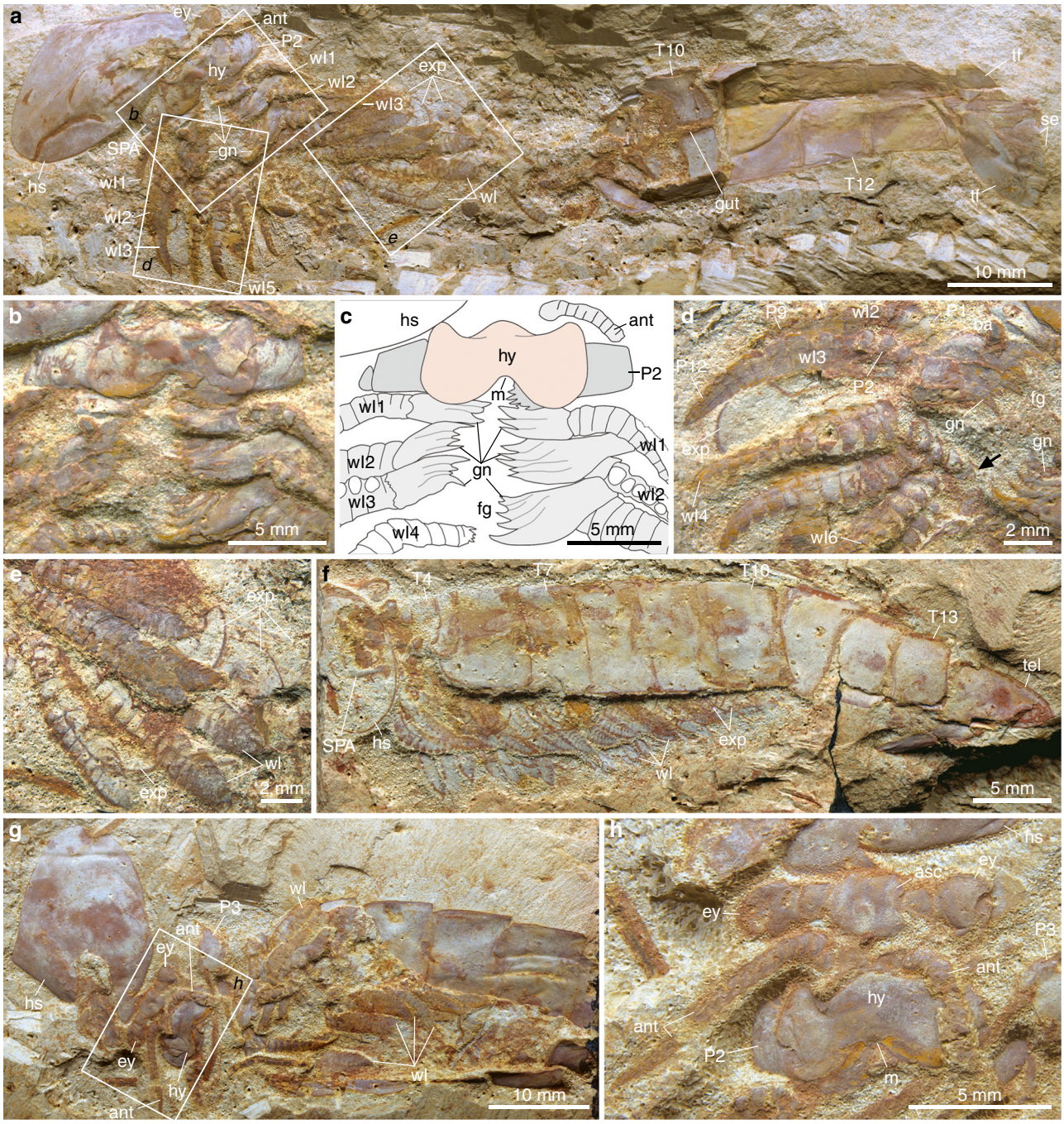

Fig. 1 *Alacaris multinoda* from the Cambrian (Stage 3) Xiaoshiba Lagerstätte. **a**–**e** YKLP 12268 (holotype). **a** Complete individual in ventral view showing disarticulated head shield, appendicular organization, trunk tergites, and tailspine with paired flukes. **b** Details of area *b*, showing antennae, hypostome, SPAs, and three sets of walking legs with differentiated gnathobasic protopodites forming a ventral food groove. **c** Interpretative drawing of **b**. **d** Close-up of area *d*, showing multisegmented endopods with prominent protopodites, followed by walking legs with spinose endites (arrowed). **e** Close-up of area *e*, showing multisegmented endopods and flap-like exopods. **f** YKLP 12269, lateral view of a complete individual. **g** YKLP 12276, specimen with disarticulated head shield, showing organization of the anterior region. **h** Close-up of area *h*, showing the anterior sclerite with stalked eyes, the insertion of the paired antennae close to the anterior edge of the hypostome, and the proximal portions of the SPAs. ant: antenna, asc: anterior sclerite, exp: exopod, ey: eye, fg: food groove, gn: gnathobase, gut: alimentary canal, hs: head shield, hy: hypostome, m: mouth, P*n:* podomeres, se: setae, SPA: specialized post-antennal appendage, tel: tailspine, tf: tail fluke, T*n:* tegites, wl*n:* walking legs

three-dimensional preservation suggest a high degree of sclerotization.

The trunk contains numerous sets of biramous limbs that gradually decrease in size posteriorly (Fig. 1). T1 to T5 have a direct correlation with the underlying appendages, but the remaining tergites are associated with up to four limb pairs as indicated by leg impressions on the exoskeleton (Fig. 1f and Supplementary Fig. 2a). T11 to T13 lack appendages (Fig. 1a, f). The distal construction of the limbs is homonomous throughout the trunk, consisting of elongate endopods with up to 16

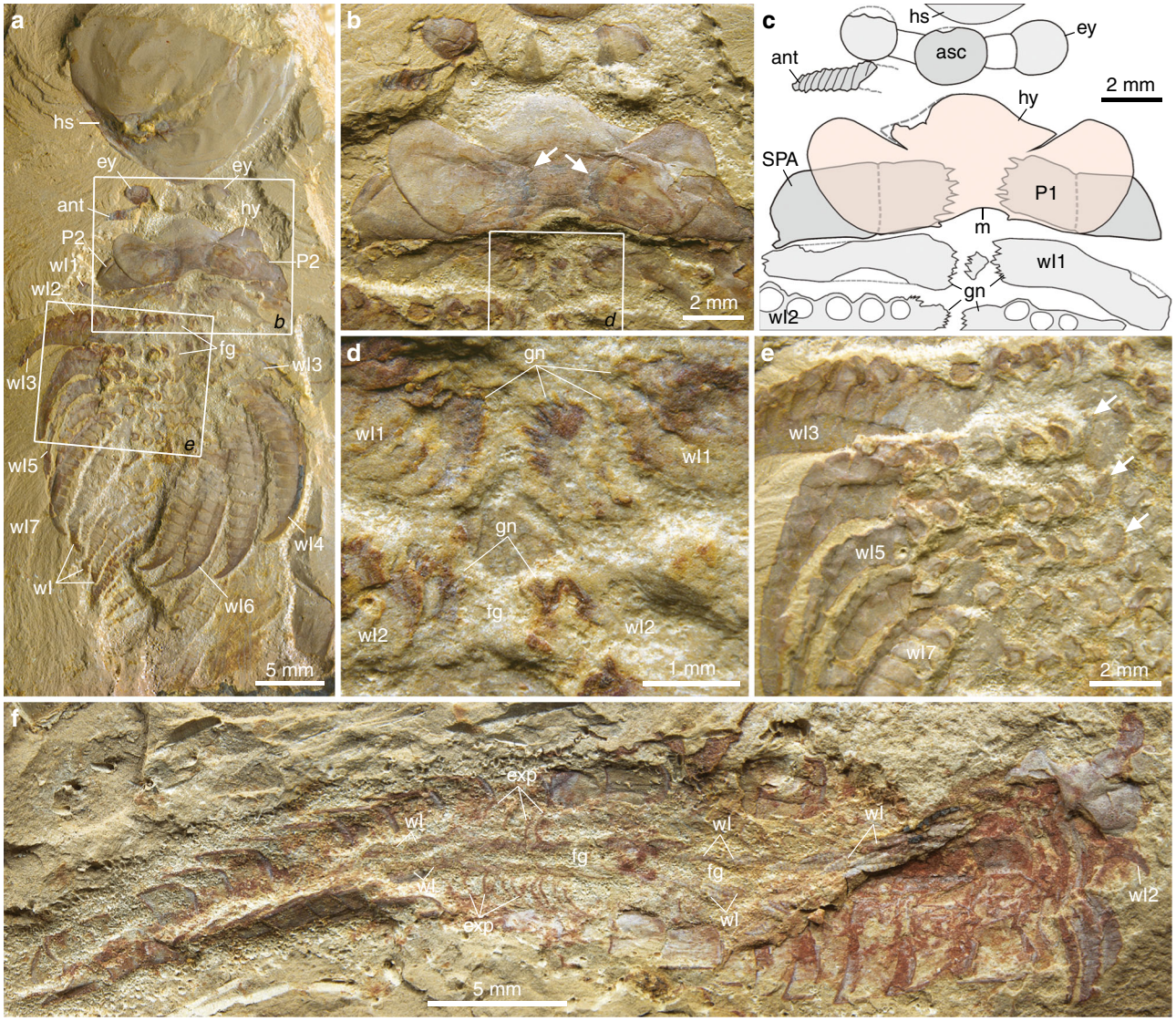

Fig. 2 *Chengjiangocaris kunmingensis* from the Cambrian (Stage 3) Xiaoshiba Lagerstätte. **a** YKLP 12307, articulated specimen in ventral view. **b** Close-up of area *b*, showing the laterally expanded hypostome that overlaps the proximal portion of the SPAs, spinose endites (arrowed) of the SPAs are visible as impressions on the overlying hypostome, and the succeeding limbs also possess gnathobases. **c** Interpretative diagram of **b**. **d** Close-up of area *d*, showing gnathobases preserved on proximal portion of limbs located behind the SPAs, forming a ventral food groove. **e** Close-up of area *e*, showing the 3rd to 7th walking legs showing proximal spinose endites (arrowed). **f** YKLP 12308, ventral view of a nearly complete individual showing the food groove present between the two rows of closely spaced walking limbs. Abbreviations as in Fig. 1

podomeres that terminate in a conical distal claw (Fig. 1a, d and Supplementary Figs 3e and 4b), and an undivided flap-shaped exopod with short marginal setae (Fig. 1a, d–f and Supplementary Fig. 4b, d). Proximally, the appendages corresponding from T1 to T3 possess a prominent antero-posteriorly compressed protopodite, with up to five dorso-ventrally aligned robust spinose endites that project towards the body midline to form a ventral groove (Fig. 1a–d and Supplementary Figs 2a–c, 3a–d). The enlarged protopodite is absent in the remaining limbs, but these also possess medially directed spinose endites (Fig. 1a–d).

New collections also illuminate the ventral morphology of the Xiaoshiba fuxianhuiids *Chengjiangocaris kunmingensis* and *Fuxianhuia xiaoshibaensis*[14,17]. The entire in situ hypostome of *C. kunmingensis* is clearly observed for the first time (Fig. 2); it closely resembles that of *A. mirabilis* (compare Fig. 1a–c and Supplementary Fig. 2c, d), including the presence of a median anterior extension delimited by slit-like furrows. However, the hypostome of *C. kunmingensis* has more developed wing-like lateral projections with rounded edges, the posterior notch is less prominent, and also flanked by a pair of short spines (Fig. 2a–c). The basal podomere of the robust SPAs carries gnathobasic edges with six spinose endites, visible as impressions through the overlying hypostome (Fig. 2b, c). At least three sets of biramous trunk limbs also have medially oriented gnathobasic edges that together form an axial ventral groove (Fig. 2d–f). Small endites are also preserved in the bases of the SPAs of *F. xiaoshibaensis* (Fig. 3e–g), although these are less prominent. The hypostome of *F. xiaoshibaensis* has a subtrapezoidal outline and bears an elevated medial region that appears to be aligned with the posterior-facing mouth opening (Fig. 3c–e); however, the posterior and lateral margins of the hypostome are broken and preclude further comparison with *Chengjiangocaris*. Neither *C. kunmingensis* nor *F. xiaoshibaensis* demonstrate the presence of enlarged protopodites as observed in *A. mirabilis* (Fig. 1a–c).

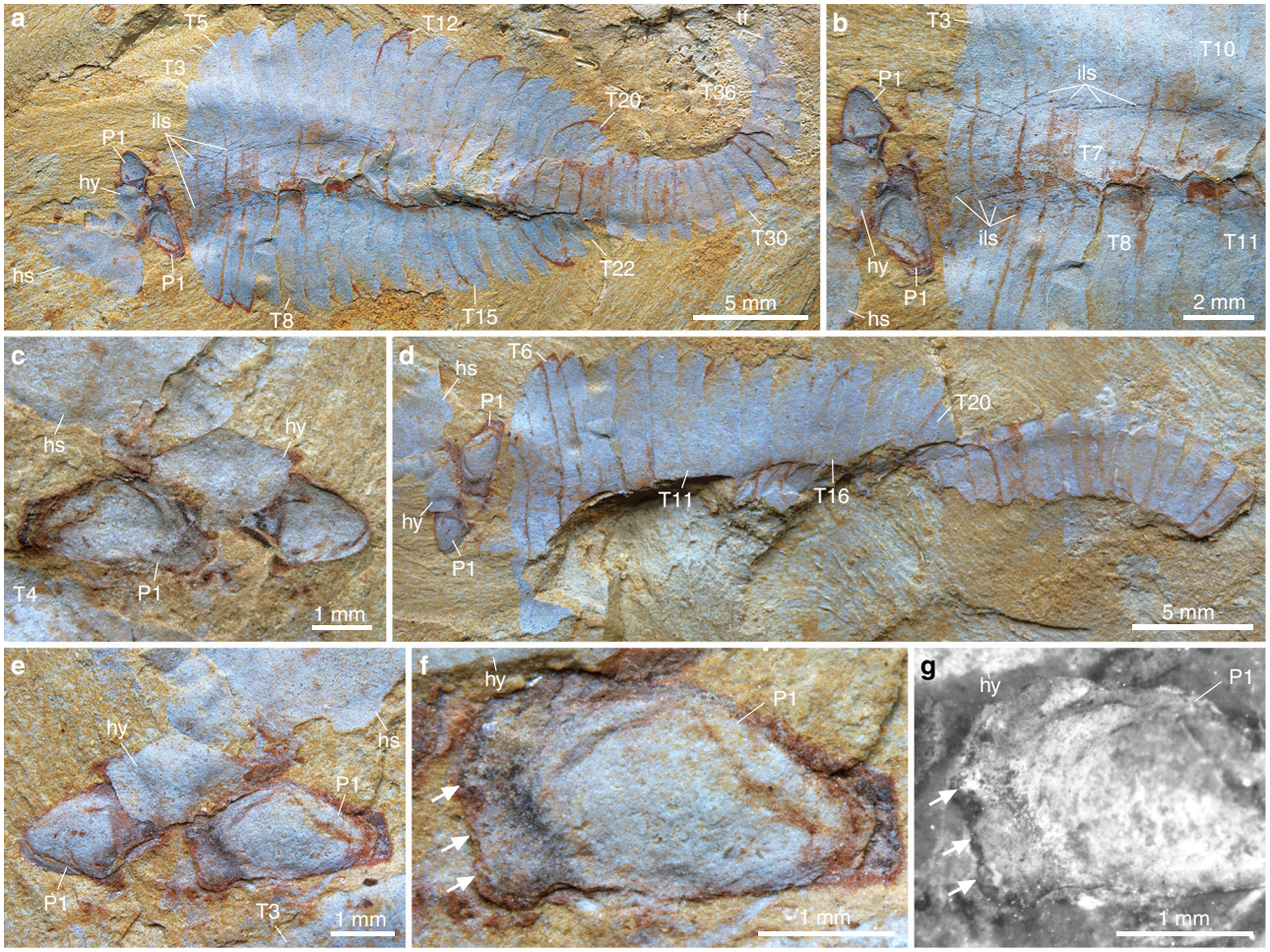

Fig. 3 *Fuxianhuia xiaoshibaensis* from the Cambrian (Stage 3) Xiaoshiba Lagerstätte. **a**–**e** YKLP 12313a: **a** a complete articulated individual; **b** close-up of **a** showing regularly occurrence of leg sheath impressions; **c** close-up of the paired P1 of SPA covered by hypostome. **d**–**g** YKLP 12313b: **d** counterpart; **e** close-up of the paired P1 of SPA covered by hypostome; **f** details of **e** showing the left P1 with partially preserved endites situated along the inner margin (arrowed); **g** fluorescence image showing endites (arrowed). Abbreviations: as in Fig. 1

Discussion

Xiaoshiba fossils provide clear evidence that the basal region of the post-deutocerebral limbs in fuxianhuiids is specialized for active gnathobasic feeding (Fig. 4). The presence of a differentiated protopodite with spinose endites indicates a predatory/scavenger autecology, in which prey would be processed by the gnathobases during the rhythmical movement of the legs, and transported along the ventral groove towards the posterior-facing mouth[1,6–8]. Food items closer to the mouth opening would be further manipulated by the interaction of the heavily sclerotized SPAs[14] and the broad posteriorly notched hypostome (Fig. 4c, d), which have a comparable organization to Palaeozoic euarthropods with a predatory/scavenger habitus[6–8,23,24]. These observations reject the prevailing view of fuxianhuiids as simple mud-feeders with exclusively locomotory trunk limbs[14,16,18,19], and instead add support to the interpretation that these stem-group euarthropods engaged, at least occasionally, in durophagous predation, as suggested by a single specimen preserved with a gut tract, which bears phosphatized midgut glands, containing fragments of eodiscoid trilobites from the Kaili biota[25]. These comparisons suggest that the feeding strategy of fuxianhuiids approximates that of the stem-group chelicerates *Sidneyia inexpectans*[6] and *Wisangocaris barbarhardyae*[26] in combining post-oral limbs with well-developed gnathobasic protopodites and evidence for shelly cololites. These observations expand the scant Cambrian record of durophagy in total-group Euarthropoda[24], without necessarily ruling out the likelihood that fuxianhuiids also preyed or scavenged on soft-bodied food items. Thus, our material illuminates the autoecology of a major clade of stem lineage representatives, and demonstrates that protopodite-based gnathobasic feeding originated earlier within the evolutionary history of total-group Euarthropoda than previously considered[5,24,27,28].

A recent re-examination of the anterior organization of the Chengjiang radiodontan *Amplectobelua symbrachiata* has revealed paired ventral structures that possess strong spinose endites with a clear masticatory function[29], which could suggest an even earlier origin for gnathobasic feeding within lower stem-group Euarthropoda[13]. Despite their striking resemblance to the proximal limb morphology of trilobites[23] and *Limulus polyphemus*[29], and the jaws of onychophorans[30], it is uncertain whether the 'gnathobasic-like structures' of *A. symbrachiata* derive from the proximal or distal region of an appendage, which obscures their homology with the gnathobasic protopodite of more crown-wards representatives (Figs. 4 and 5). Given that the dorsal and ventral limb elements of radiodontans were not fused into a single biramous appendage[31], the 'gnathobasic-like structures' of *A. symbrachiata* cannot possibly derive from the protopodite in the traditional sense[3]. Instead, we regard the structures of *A. symbrachiata* as independently modified limbs for

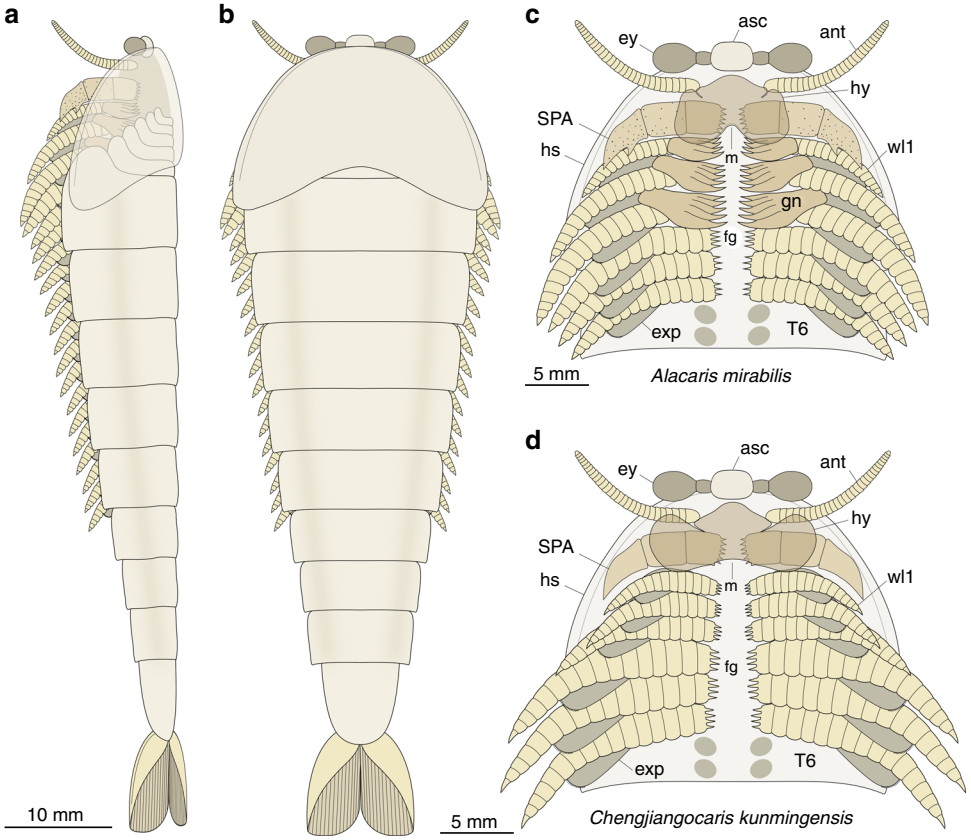

Fig. 4 Morphological reconstruction of *Alacaris mirabilis* and *Chengjiangocaris kunmingensis*. **a** Full-body reconstruction of *A. mirabilis* in lateral view. **b** Full-body reconstruction of *A. mirabilis* in dorsal view. **c** Ventral view of the head and anterior trunk region of *A. mirabilis* showing gnathobasic protopodite ventral food groove. **d** Ventral view of the head and anterior trunk region of *C. kunmingensis*; note the differences in the morphology of the hypostome relative to *A. mirabilis*, and the presence of smaller gnathobasic endites on the proximal limbs. Abbreviations as in Fig. 1

food processing that worked in conjunction with the oral cone and the sclerotized frontal appendages, and which most likely originated through an analogous process of cephalization similar to that observed in other lineages within Panarthropoda[22].

The results of a phylogenetic analysis (Supplementary Fig. 5, Supplementary Note 1) resolve Fuxianhuiida as a monophyletic group within upper stem-group Euarthropoda[13] (Fig. 5a), placed a node above a paraphyletic grade of Cambrian bivalved forms (e.g., refs. [27,32,33]; contra [5,10,16,34]), and as sister group to a clade that includes megacheirans[28,35] and artiopodans[6,8,16,23]. These results inform the step-wise evolution of PD limb differentiation along the euarthropod stem lineage. The post-deutocerebral appendages of bivalved euarthropods—which comprise the most basal representatives of Deuteropoda[13,36]—consist of a series of flap-like exopod with marginal setae, and multipodomerous endopods; however, the structure of the proximal podomeres is generally obscured by the overlying carapace. In stem-wards forms, such as *Jugatacaris agilis*[32] and *Nereocaris* species[27,33], the slender endopods are composed of up to 30 homonomous podomeres with short endites that show no PD differentiation (Fig. 5b). More crown-wards representatives, like *Canadaspis perfecta*[37], show a slightly higher degree of limb specialization. The robust trunk endopods of *C. perfecta* consist of at least 11 freely articulating podomeres; those in the proximal half of the endopod bear endites with delicate comb-like terminations, whereas the endites on the seven distal-most podomeres are shorter and unbranched (Fig. 5b). However, the bivalved carapace of *C. perfecta* obscures the basal portion of the biramous appendages, and thus the organization of the protopodite is unknown (sensu ref. [37]; contra ref. [34]). A recent appraisal of the trunk appendage morphology in the Burgess Shale bivalved euarthropods *Odaraia alata*[38], *Branchiocaris pretiosa*[39], and *Tokummia katalepsis*[34] suggests the presence of a segmented protopodite associated with an endopod with seven podomeres (see basipod in ref. [34]), which would imply a deeper origin for PD limb differentiation according to our topology (Fig. 5a; Supplementary Fig. 5). Evidence supporting the presence of a specialized protopodite in these taxa is contentious, however, as there is little structural PD distinction in the trunk appendages of these three taxa, other than the difference in width that can be expected along the length of the limbs[34,38,39]. The putative protopodite of *T. katalepsis* clearly displays complete transverse segmental boundaries that are morphologically indistinguishable from those defining the distal podomeres that constitute the endopod (see Figs. 1c, 2d, h, i, m, and extended data fig. 9h in ref. [34]). Although the putative protopodite of *T. katalepsis* is reconstructed as having more robust endites than the endopod, the figured fossil material demonstrates that the endopod podomeres possess similar endites as those observed in the proximal limb region, and thus show no signs of this proposed regionalization (compare figs. 1d and 3c in ref. [34]). The lack of substantial PD differentiation is more evident in *O. alata* (see extended fig. 9g, h in ref. [34]), as the limb portion regarded as the protopodite is again morphologically identical to the distal endopod—albeit slightly thicker—and also possesses complete transverse segmental boundaries. Finally, none of the figured material of *B. pretiosa* (see fig. 1i and extended data fig. 7e in ref. [34]) provides clear evidence of a differentiation between the proximal and distal portions of the trunk limbs. As such, the proximal limb organization of *O. alata*[38], *B. pretiosa*[39], and *T. katalepsis*[34] fundamentally differs from the

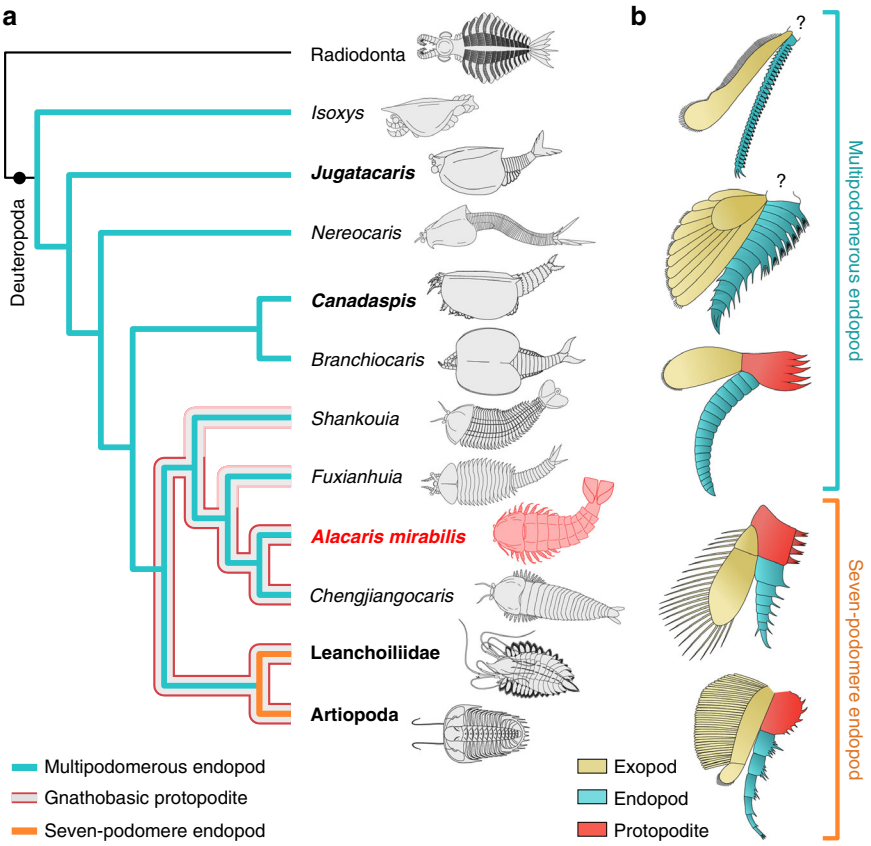

Fig. 5 Evolution of euarthropod PD limb axis differentiation. **a** Simplified cladogram showing phylogenetic position of *Alacaris mirabilis*, origin of the gnathobasic protopodite, and evolutionary reduction in the number of endopod podomeres within stem-group Euarthropoda (detailed results presented in Supplementary Fig. 5b); the presence of gnathobasic protopodites on the trunk limbs of *Alacaris* and *Chengjiangocaris* suggests their possible occurrence in other fuxianhuiid taxa for which proximal limb data are not currently available. **b** Post-deutocerebral appendage organization and homology among stem and crown-group euarthropods. Limb reconstructions correspond to taxa highlighted in bold in **a**, ordered from top to bottom

morphologically and functional specialized compressed protopodite without segmental boundaries expressed in *A. mirabilis* (Figs. 1a–c, 4, 5).

The post-deutocerebral appendages of *A. mirabilis* represent the earliest occurrence of substantial PD differentiation within the euarthropod stem lineage, expressed in the discrete basal protopodite with up to five spinose endites combined with a multipodomerous distal endopod with a relatively simple construction (Figs. 4 and 5b). The presence of multipodomerous endopods is resolved as a symplesiomorphy of upper stem-group Euarthropoda[13], which argues against the interpretation of fuxianhuiid limbs as being structurally comparable relative to the those of lobopodians, which lack epidermal segmentation, sclerotized plates, flexible articulating membranes, and substantial PD differentiation (contra refs. [5,16,18,19]; see also ref. [40]). The analysis also indicates that the origin of the protopodite preceded the evolutionary reduction in the number of endopod podomeres (Fig. 5a), from more than a dozen in upper stem-group euarthropods[13,14,18,27,32,33,40] to seven (or fewer) in more crown-wards representatives such as megacheirans and artiopodans[3,5–8,16,23,28] (Fig. 5b). This result falsifies hypotheses in which the protopodite and the seven-podomere endopod evolved simultaneously from the fusion of the proximal podomeres in Cambrian stem-group representatives (sensu refs. [5,11]), and is better reconciled with gene expression data that suggest a possible developmental partition between the protopodite and the distal portions of the limb[2,3,9,41,42].

The differentiated protopodite constitutes an archetypical feature of the post-deutocerebral appendages in extinct taxa that occupy a crown-wards position relative to fuxianhuiids[6–8,18,23,28,35] (Fig. 5a), as well as crown-group chelicerates[7,43] and mandibulates[3,4,44,45]. Thus, Xiaoshiba fuxianhuiids pinpoint the origin of the fundamental PD appendicular organization, and ancestral gnathobasic mode of feeding, that define the early evolution of the crown-group[1,3,5,40,45] as well as the foundations for the remarkable ecomorphological diversity of mouthparts observed in extant Euarthropoda[2,9,41].

Methods

Fossil repository and imaging. Fossil material is deposited at the Key Laboratory for Palaeobiology, Yunnan University, Kunming, China. Specimens were photographed with a Nikon D3X fitted with a Nikon AF-S Micro Nikkor 105 mm lens, and a LEICA M205-C stereomicroscope fitted with a Leica DFC 500 digital camera with directional illumination provided by a LEICA LED5000 MCITM. Fluorescent photography was performed using a LEICA DFC 7000T monochrome digital camera (fitted with a LEICA 10450028 lens) attached to a LEICA M205 FA fluorescence stereomicroscope (green-orange fluorescence).

Phylogenetic analysis. The dataset (Supplementary Notes 1 and 2), consisting of 43 taxa and 84 characters, was analyzed using the freely available phylogenetic software TNT[46] (tree analysis using new technology) v.1.1. Analyses were performed using New Technology Search with Parsimony Ratchet[47], Sectorial Searches, Tree Drifting, and Tree Fusing[48], set to find the shortest tree 100 times. The analysis was first run under equal weights (Supplementary Fig. 5a), and a second iteration under implied weights with a concavity value of three (Supplementary Fig. 5b). See refs. [30] for a discussion on the applicability and utility of character weighting in phylogenetic analyses.

Nomenclatural acts. This published work and the nomenclatural acts it contains have been registered in ZooBank, the proposed online registration system for the International Code of Zoological Nomenclature (ICZN). The ZooBank LSIDs

(Life Science Identifiers) can be resolved and the associated information viewed through any standard web browser by appending the LSID to the prefix 'http://zoobank.org/'. The LSID for this publication is: urn:lsid:zoobank.org:act:E2B329EC-560B-463B-AC94-5E4F638F7A1A.

Data availability. The character dataset (Supplementary Notes 1 and 2) is available as supplementary information. Photographic material of the fossils is available from the authors upon request. Studied specimens are deposited at the Yunnan Key Laboratory for Palaeobiology, Yunnan University, Kunming.

Received: 24 September 2017 Accepted: 26 December 2017
Published online: 01 February 2018

References

1. Wyse, G. A. & Dwyer, N. K. The neuromuscular basis of coxal feeding and locomotory movements in *limulus*. *Biol. Bull.* **144**, 567–579 (1973).
2. Scholtz, G., Mittmann, B. & Gerberding, M. The pattern of Distal-less expression in the mouthparts of crustaceans, myriapods and insects: new evidence for a gnathobasic mandible and the common origin of mandibulata. *Int. J. Dev. Biol.* **42**, 801–810 (2004).
3. Boxshall, G. A. The evolution of arthropod limbs. *Biol. Rev.* **79**, 253–300 (2004).
4. Zhang, X.-G., Siveter, D. J., Waloszek, D. & Maas, A. An epipodite-bearing crown-group crustacean from the lower Cambrian. *Nature* **449**, 595–598 (2007).
5. Waloszek, D., Maas, A., Chen, J.-Y. & Stein, M. Evolution of cephalic feeding structures and the phylogeny of arthropoda. *Palaeogeogr. Palaeoclimatol. Palaeoecol.* **254**, 273–287 (2007).
6. Zacaï, A., Vannier, J. & Lerosey-Aubril, R. Reconstructing the diet of a 505-million-year-old arthropod: *Sidneyia inexpectans* from the burgess shale fauna. *Arthropod Struct. Dev.* **45**, 200–220 (2016).
7. Selden, P. A. Functional morphology of the prosoma of *Baltoeurypterus tetragonophthalmus* (fischer) (chelicerata: eurypterida). *Trans. R. Soc. Edinb. Earth Sci.* **72**, 9–48 (1981).
8. Fortey, R. A. & Owens, R. M. Feeding habits in trilobites. *Palaeontology* **42**, 429–465 (1999).
9. Abzhanov, A. & Kaufman, T. C. Homologs of *Drosophila* appendage genes in the patterning of arthropod limbs. *Dev. Biol.* **227**, 673–689 (2000).
10. Waloszek, D. Cambrian "Orsten"-type preserved arthropods and the phylogeny of Crustacea. in *The New Panorama of Animal Evolution: Proceedings of the 18th International Congress of Zoology* (eds Legakis, A., et al.) 66–84 (Pensoft Publ., Sofia-Moscow, 2003).
11. Itô, T. Origin of the basis in copepod limbs, with reference to remipedian and cephalocarid limbs. *J. Crust. Biol.* **9**, 85–103 (1989).
12. Yang, J. et al. A superarmored lobopodian from the Cambrian of China and early disparity in the evolution of onychophora. *Proc. Natl. Acad. Sci. USA* **112**, 8678–8683 (2015).
13. Ortega-Hernández, J. Making sense of 'lower' and 'upper' stem-group Euarthropoda, with comments on the strict use of the name Arthropoda von Siebold, 1848. *Biol. Rev.* **91**, 255–273 (2016).
14. Yang, J., Ortega-Hernández, J., Butterfield, N. J. & Zhang, X.-G. Specialized appendages in fuxianhuiids and the head organization of early euarthropods. *Nature* **494**, 468–471 (2013).
15. Hou, X.-G. & Bergström, J. in *The Early Evolution of Metzoan and the Significance of Problematic Taxa* (eds Simonetta, A. M. & Conway Morris, S.) 179–187 (Cambridge Univ. Press, Cambridge, 1991).
16. Hou, X.-G. & Bergström, J. Arthropods of the lower Cambrian Chengjiang fauna, southwest China. *Foss. Strat.* **45**, 1–116 (1997).
17. Yang, J. et al. Fuxianhuiid ventral nerve cord and early nervous system evolution in panarthropoda. *Proc. Natl. Acad. Sci. USA* **113**, 2988–2993 (2016).
18. Waloszek, D., Chen, J.-Y., Maas, A. & Wang, X.-Q. Early Cambrian arthropods—new insights into arthropod head and structural evolution. *Arthropod Struct. Dev.* **34**, 189–205 (2005).
19. Bergström, J., Hou, X.-G., Zhang, X.-G., Liu, Y. & Clausen, S. A new view of the Cambrian arthropod. *Fuxianhuia. GFF* **130**, 189–201 (2008).
20. Li, S.-J., Kang, C.-L. & Zhang, X.-G. Sedimentary environment and trilobites of lower Cambrian Yuxiansi formation in Leshan District. *Bull. Chengdu Inst. Geol. Min. Resour., Chin. Acad. Geol. Sci.* **12**, 37–56 (1990). [in Chinese].
21. Ma, X.-Y., Edgecombe, G. D., Hou, X.-G., Goral, T. & Strausfeld, N. J. Preservational pathways of corresponding brains of a Cambrian euarthropod. *Curr. Biol.* **25**, 2969–297 (2015).
22. Ortega-Hernández, J., Budd, G. E. & Janssen, R. Origin and evolution of the panarthropod head–a palaeobiological and developmental perspective. *Arthrop. Struct. Dev.* **46**, 354–379 (2017).
23. Zeng, H., Zhao, F.-C., Yin, Z.-J. & Zhu, M.-Y. Appendages of an early Cambrian metadoxidid trilobite from Yunnan, SW China support mandibulate affinities of trilobites and artiopods. *Geol. Mag.* **154**, 1306–1328 (2017).
24. Bicknell, R. D. C. & Paterson, J. R. Reappraising the early evidence of durophagy and drilling predation in the fossil record: implications for escalation and the Cambrian explosion. *Biol. Rev*. in press (https://doi.org/10.1111/brv.12365).
25. Zhu, M.-Y., Vannier, J., Iten, H. V. & Zhao, Y.-L. Direct evidence for predation on trilobites in the Cambrian. *Proc. R. Soc. Lond. B* **271**, S277–S280 (2004). (Suppl. 5).
26. Jago, J. B., García-Bellido., D. C. & Gheling, J. B. An early Cambrian chelicerate from the Emu Bay Shale, South Australia. *Palaeontology* **59**, 549–562 (2016).
27. Legg, D. A., Sutton, M. D., Edgecombe, G. D. & Caron, J.-B. Cambrian bivalved arthropod reveals origin of arthrodization. *Proc. R. Soc. B* **279**, 4699–4704 (2012).
28. Aria, C., Caron, J.-B. & Gaines, R. A large new leanchoiliid from the Burgess Shale and the influence of inapplicable states on stem arthropod phylogeny. *Palaeontology* **58**, 629–660 (2015).
29. Cong, P.-Y., Daley, A. C., Edgecome, G. D. & Hou, X.-G. The functional head of the Cambrian radiodontan (stem-group euarthropoda) *Amplectobelua symbrachiata*. *BMC Evol. Biol.* **17**, 208 (2017).
30. Smith, M. R. & Ortega-Hernández, J. *Hallucigenia*'s onychophoran-like claws and the case for tactopoda. *Nature* **514**, 363–366 (2014).
31. Van Roy, P., Daley, A. C. & Briggs, D. E. G. Anomalocaridid trunk limb homology revealed by giant filter-feeder with paired flaps. *Nature* **522**, 77–80 (2015).
32. Fu, D.-J. & Zhang, X.-L. A new arthropod *Jugatacaris agilis* n. gen. n. sp. from the early Cambrian Chengjiang biota, South China. *J. Paleontol.* **85**, 567–586 (2011).
33. Legg, D. A. & Caron, J.-B. New middle Cambrian bivalved arthropods from the burgess shale (British Columbia, Canada). *Palaeontology* **57**, 691–711 (2014).
34. Aria, C. & Caron, J. B. Burgess Shale fossils illustrate the origin of the mandibulate body plan. *Nature* **545**, 89–92 (2017).
35. Haug, J. T., Briggs, D. E. G. & Haug, C. Morphology and function in the Cambrian Burgess Shale megacheiran arthropod *Leanchoilia superlata* and the application of a descriptive matrix. *BMC Evol. Biol.* **12**, 162 (2012).
36. Legg, D. A., Sutton, M. D. & Edgecombe, G. D. Arthropod fossil data increase congruence of morphological and molecular phylogenies. *Nat. Commn.* **4**, 2485 (2013).
37. Briggs, D. E. G. The morphology, mode of life, and affinities of *Canadaspis perfecta* (crustacea: phyllocarida), middle Cambrian, burgess shale, British Columbia. *Philos. Trans. R. Soc. Lond. B* **281**, 439–487 (1978).
38. Briggs, D. E. G. The arthropod *Odaraia alata* walcott, middle Cambrian, burgess shale, British Columbia. *Philos. Trans. R. Soc. Lond. B* **291**, 541–582 (1981).
39. Briggs, D. E. G. The arthropod *Branchiocaris* n. gen., middle Cambrian, burgess shale, British Columbia. *Geol. Surv. Can. Bull.* **264**, 1–17 (1976).
40. Budd, G. E. Tardigrades as 'Stem-group Arthropods': the evidence from the Cambrian fauna. *Zool. Anz.* **240**, 265–279 (2001).
41. Williams, T. A., Nulsen, C. & Nagy, L. M. A complex role for distal-less in crustacean appendage development. *Dev. Biol.* **241**, 302–312 (2002).
42. Jockusch, E. L. Developmental and evolutionary perspectives on the diversification of arthropod appendages. *Integ. Comp. Biol.* **57**, 533–545 (2017).
43. Briggs, D. E. G. et al. Silurian horseshoe crab illuminates the evolution of arthropod limbs. *Proc. Natl. Acad. Sci. USA* **109**, 15702–15705 (2012).
44. Harvey, T. H. P. & Butterfield, N. J. Sophisticated particle-feeding in a large early Cambrian crustacean. *Nature* **452**, 868–871 (2008).
45. Harvey, T. H., Vélez, M. I. & Butterfield, N. J. Exceptionally preserved crustaceans from western Canada reveal a cryptic Cambrian radiation. *Proc. Natl. Acad. Sci. USA* **109**, 1589–1594 (2012).
46. Goloboff, P. A., Farris, J. S. & Nixon, K. C. TNT, a free program for phylogenetic analysis. *Cladistics* **24**, 774–786 (2008).
47. Nixon, K. C. The parsimony ratchet, a new method for rapid parsimony analysis. *Cladistics* **15**, 407–414 (1999).
48. Goloboff, P. A. Analysing large data sets in reasonable times: Solutions for composite optima. *Cladistics* **15**, 415–428 (1999).
49. Congreve, C. R. & Lamsdell, J. C. Implied weighting and its utility in palaeontological datasets: a study using modelled phylogenetic matrices. *Palaeontology* **59**, 447–462 (2016).

Acknowledgements

We thank K.-S. Du, J.-F. He, and K.-R. Li for assistance with fossil collection. This study was funded by the National Natural Science Foundation of China (U1402232, 41472022 and 41730318 to X.-G.Z. and J.Y.), Herchel-Smith Postdoctoral Fellowship and

Emmanuel College Bye-Fellowship, University of Cambridge (to J.O.-H.), and Department of Science and Technology, Yunnan Province (2015HA045 to X.-G.Z.).

Author contributions

X.-g.Z. and J.Y. conceived the study. J.Y., T.L., and J.-b.H. collected the material. J.Y. prepared all specimens for photography. J.O.-H., and X.-g.Z. performed research, and wrote the manuscript with input from other authors. X.-g.Z. and J.O.-H prepared the figures. D.A.L. designed and performed the phylogenetic analysis. All authors discussed and approved the manuscript.

Additional information

Supplementary Information accompanies this paper at https://doi.org/10.1038/s41467-017-02754-z.

Competing interests: The authors declare no competing financial interests.

Reprints and permission information is available online at http://npg.nature.com/reprintsandpermissions/

Publisher's note: Springer Nature remains neutral with regard to jurisdictional claims in published maps and institutional affiliations.

Supplementary Information

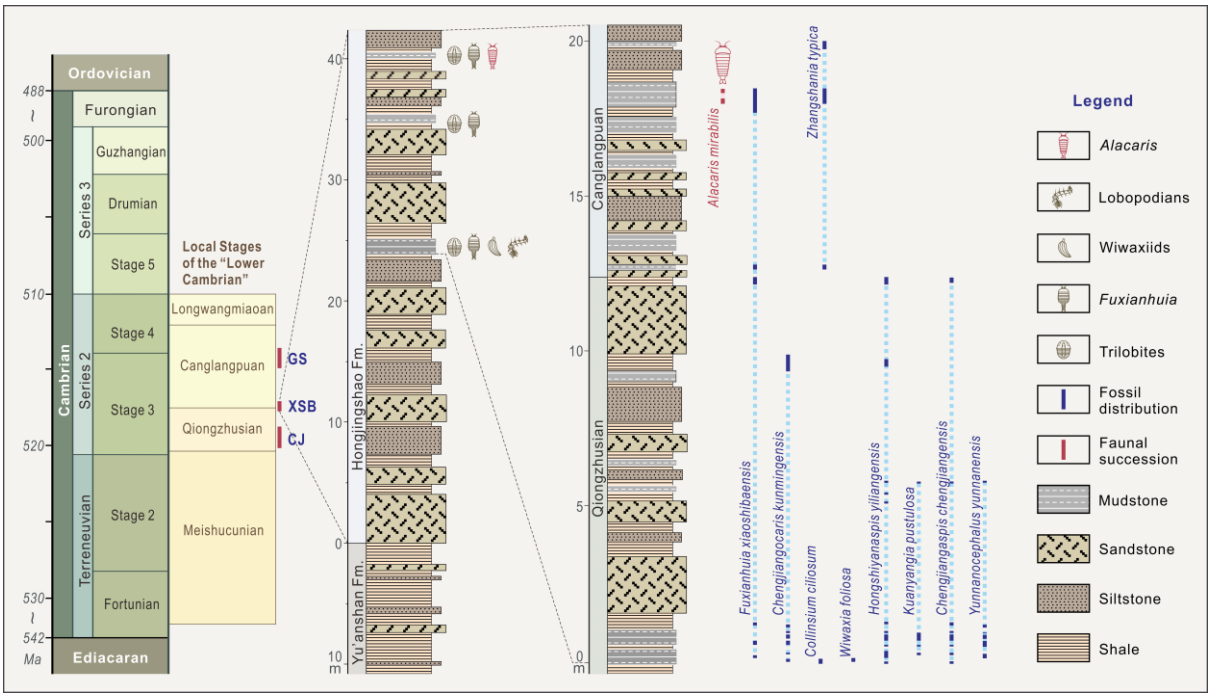

Supplementary Figure 1 | Stratigraphic column and fossil distribution within the Cambrian (Stage 3) Hongjingshao Formation, Xiaoshiba section, Kunming. *Alacaris mirabilis* is found in mudstone about 10 meters above the fossil assemblage of *Yunnanocephalus–Chengjiangaspis–Hongshiyanaspis* biozone[1–3]. According to the coexisting trilobite *Zhangshania*, *Alacaris mirabilis* occurs at the bottom of the Canglangpuan. Geologically the horizon of the Xiaoshiba Lagersttäte (XSB) is above the Chengjiang (CJ) and below the Guanshan (GS) biotas.

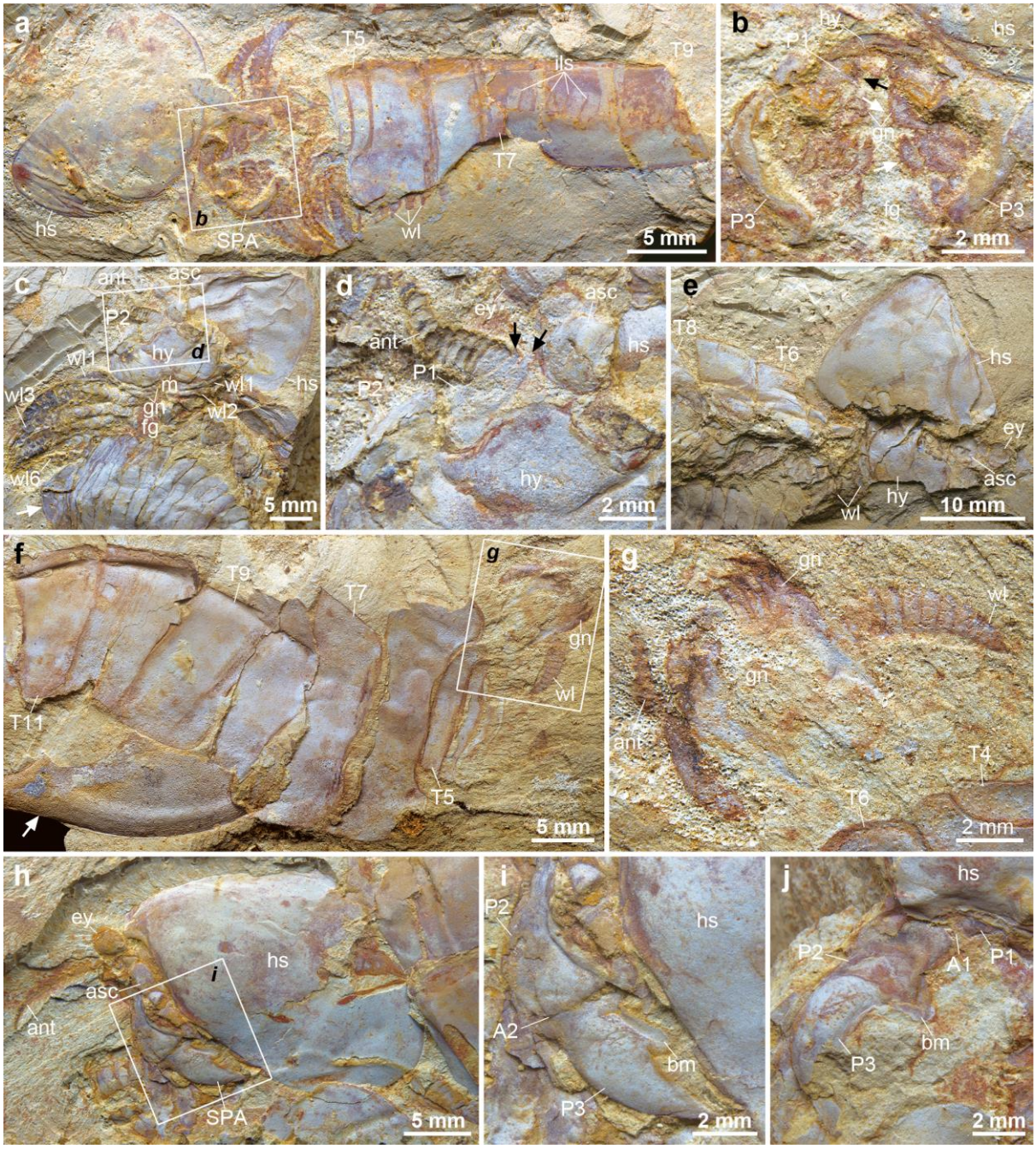

Supplementary Figure 2 | *Alacaris mirabilis* from the Cambrian (Stage 3) Xiaoshiba Lagerstätte. (**a**) YKLP 12276, ventral view of a partially disarticulated specimen showing the anterior appendicular organization. (**b**) Close-up of area *b*, showing overall organization of the SPAs, fine spinose endites along the inner basal margin of the SPAs (black arrow) and gnathobases of the post-oral appendages (white arrow). (**c**) YKLP 12310a, anterior portion of individual preserved in ventral view ventral view, buried alongside articulated tergites of *Fuxianhuia* sp. (white arrow). (**d**) Close-up of area *d*, showing stalked eyes, antenna and hypostome. (**e**) YKLP 12310b, counterpart showing fragmentary head shield and tergites. (**f**) YKLP 12311, anterior portion of an incomplete individual together, preserved alongside a trilobite librigena (arrowed). (**g**) Close-up of area *g*, showing antenna and gnathobases with strong spinose endites. (**h**) YKLP 12272, anterior portion of an individual preserved in lateral view showing stalked eye, an antenna, and the left SPA. (**i**) Enlargement of area *i*, showing details of the SPA, which is ornamented with fine nods, showing articulation and marginal

blade. (**j**) YKLP 12273, a SPA showing blade-like inner margin and articulation. Abbreviations: A*n*, articulations; ant, antenna; asc, anterior sclerite; bm, blade-like margin; ey, eye; fg, food groove; gn, gnathobase; hs head shield; hy, hypostome; ils, impression of leg sheath; m, mouth; P*n*, podomeres; SPA, specialized post-antennal appendage; T*n*, tegites; wl*n*, walking legs.

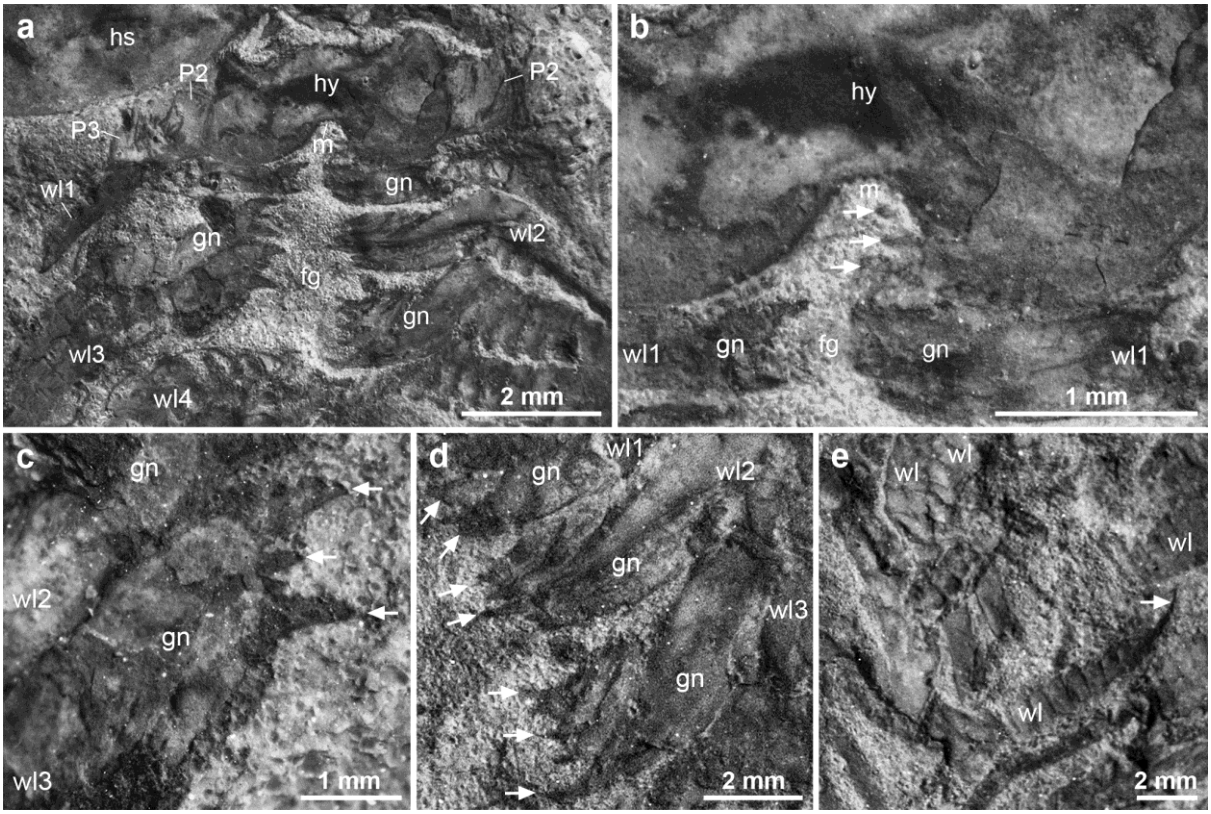

Supplementary Figure 3 | Composite-fluorescence illustrations of feeding apparatus in *Alacarus mirabilis* from the Cambrian (Stage 3) Xiaoshiba Lagerstätte. (**a**) YKLP 12268 (holotype), ventral view revealing the hypostome overlying the basal portions of the SPAs, and the differentiated gnathobasic protopodite with strong spinose endites. (**b**) Close-up of (a), showing posterior notch in the hypostome that most likely accommodated the posterior-facing mouth opening; note the preservation of spinose endites (white arrow) of the SPAs underneath the hypostome. (**c**) Details of (**a**) showing the fine spinose endites of varying in size (arrowed) of the third head limb on the right side. (**d**) Well-preserved gnathobases on the left side. (**e**) YKLP 12275, detail of walking legs with a long distal spine (arrowed). Abbreviations: as in Supplementary Figure 2.

Supplementary Figure 4 | Dorsal exoskeleton of *Alacaris mirabilis* from the Cambrian (Stage 3) Xiaoshiba Lagerstätte. (**a**) YKLP 12271, large individual with slightly displaced cephalic shield and articulated trunk tergites. (**b**) Close-up of area *b*, showing anterior walking legs on the right side. (**c**) YKLP 12277, complete specimen preserved in lateral view, showing full tergite count; note the presence of five anterior reduced tergites. The leg sheath impressions indicate the presence of several pairs of limbs per tergite, and suggest the absence of limbs on the posterior tergites. (**d**) YKLP 12312, anterior portion of a fragmentary individual showing preserved endopods and exopods of walking limbs. (**e**) YKLP 12268b, counterpart of the type specimen with only the paired tail flukes preserved. Abbreviations: se, setae; tel, tail spine; tf, tail fluke; others as in Supplementary Figure 2.

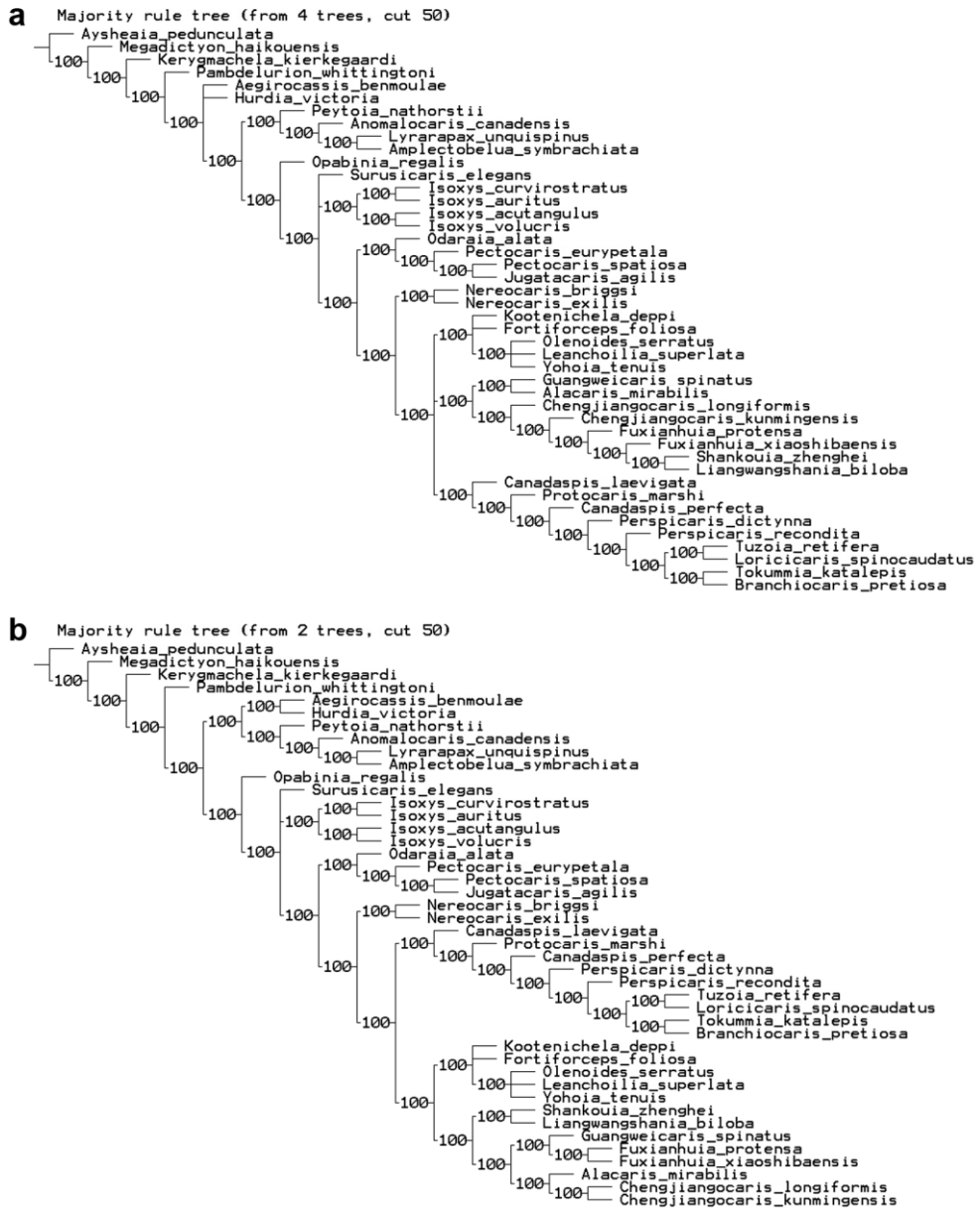

Supplementary Figure 5 | Phylogenetic position of *Alacaris mirabilis* in the context of total-group Euarthropoda. (**a**) Majority rule consensus of four most parsimonious trees calculated under equal weights. (**b**) Majority rule consensus of two most parsimonious trees calculated under implied weights (*k*=3).

Supplementary Note 1 | Systematic Palaeontology

(upper stem-group) Euarthropoda Lankester, 1904 (see discussion in ref.4)

Fuxianhuiida Bousfield,1995[5]

Constituent taxa. *Shankouia zhenghei* Walozsek *et al.*, 2005[6] (Cambrian Stage 3, Chengjiang); *Liangwangshania biloba* Chen, 2005[7] (Cambrian Stage 3, Chengjiang); Fuxianhuiidae Hou and Bergström, 1997[8] (Cambrian Stage 3, Chengjiang, Xiaoshiba and Guanshan); Chengjiangocarididae Hou and Bergström, 1997[8] (Cambrian Stage 3, Chengjiang and Xiaoshiba).

Emended diagnosis. Euarthropods with unfused subtrapezoidal head shield articulated with an anterior sclerite associated with stalked compound eyes. Trunk consists of broadly overlapping tergites that taper in width posteriorly. Variable number of anteriormost reduced tergites concealed under head shield in life position. Pre-oral first appendage pair antenniform, composed of up to 20 podomeres. Para-oral second appendage pair robust, consisting of three podomeres with acute distal termination. Sclerotized hypostome covers mouth opening as proximal bases of second limb pair. Trunk limbs biramous, with homonomous construction throughout body. Up to four limb pairs are associated with each trunk tergite. Endopod consists of approximately 12 podomeres. Differentiated gnathobasic protopodite confirmed only in some species. Exopod oval-shaped, fringed with short marginal setae. Tail spine conical or paddle-shaped, frequently associated with paired tail flukes. Revised from ref. 8.

Remarks. The monophyly of Fuxianhuiida Bousfield, 1995[5] is supported by several synapormorphies, and further confirmed by the results of the phylogenetic analysis (Supplementary Fig. 5). The proposed emended diagnosis provides a more accurate depiction of the morphological characters that define Fuxianhuiida relative to previous studies that have addressed the classification of this clade[5,8]. *Shankouia zhenghei* Waloszek*et al.*, 2005[6], and *Liangwangshania biloba* Chen, 2005[7], cannot be accommodated into either of the existing families based on their morphology (*contra* ref. 7). Although both of these taxa possess an elongate trunk with expanded tergopleurae that taper posteriorly and a paddle-shaped tail spine, the results of the phylogenetic analysis does not support their monophyly into a clade (Supplementary Fig. 5), but rather as basally branching members within Fuxianhuiida.

Fuxianhuiidae Hou and Bergström, 1997[8]

= Guangweicaridaec Luo *et al.*, 2007[9]

Constituent taxa. *Fuxianhuia protensa*Hou, 1987[10] (Cambrian Stage 3, Chengjiang); *Fuxianhuia xiaoshibaensis* Yang *et al.*, 2013[2] (Cambrian Stage 3, Xiaoshiba); *Guangweicaris spinatus* Luo *et al.*, 2007[9] (Cambrian Stage 3, Guanshan).

Emended diagnosis. Fuxianhuiids with subtrapezoidal head shield with approximately 1:4 length/width ratio, covering three anteriormost reduced tergites. Trunk subidivided into two morphologically distinct regions, consisting of anterior limb-bearing thorax with well-developed expanded tergopleurae, and narrow limb-less abdomen with ring-like tergites. Endopods of biramous limbs with rounded termination; endopods short in length, not reaching beyond the thoracic tergite and head shield margins.

Remarks. The close morphological similarities shared between *Fuxianhuia* species[2,8,11] and *Guangweicaris*—particularly the presence of three reduced tergites and the differentiation of the trunk into a thoracic and abdominal regions—support their classification within Fuxianhuiidae. We follow Yang[12] in recognizing Guangweicaridaidae Luo *et al.*, 2007[9], as a synonym of FuxianhuiidaeHou and Bergström, 1997[8].

Chengjiangocaridaidae Hou and Bergström, 1997[8]

Constituent taxa. *Chengjiangocaris longiformis* Hou and Bergström, 1991[13] (Cambrian Stage 3, Chengjiang); *Chengjiangocaris kunmingensis* Yang *et al.*, 2013[2] (Cambrian Stage 3, Xiaoshiba); *Alacaris mirabilis* gen. et sp. nov. (Cambrian Stage 3, Xiaoshiba).

Emended diagnosis. Fuxianhuiids with subtrapezoidal heart-shaped head shield with approximately 1:1 length/width ratio, covering five anteriormost reduced tergites. Trunk tergites gradually taper in width posteriorly. Biramous limbs present throughout most of trunk, except for posteriormost tergites. Endopod of biramous limbs well-developed, terminating in conical tip. Enodpods elongate, frequently reaching beyond trunk tergite and head shield margins.

Remarks. *Alacaris mirabilis*is confidently recognized as a member of Chengjiangocaridaidae Hou and Bergström[8] based on the presence of five anteriormost reduced trunk tergites, the dimensions of the head shield, a posterior tapering trunk, and the morphology of the endopods. The main differences between *Alacaris* and *Chengjiangocaris* species[2,8,13] are expressed in the number of trunk tergites and the presence of a well-developed protopodite in the former taxon.

Supplementary Note 2 | Character coding

Continuous characters

Cephalic (carapace)

0. *Length to width ratio of anterior sclerite*.

Inapplicable for taxa lacking a distinct anterior sclerite (Character 17). An elongate anterior sclerite, compared to width, is seen in the hurdids, specifically *Hurdia victoria*, and *Aegirocassis benmoulae*, whilst the anomalocaridids, and upper-stem-group euarthropods have an anterior sclerite that is wider than long.

1. *Tallest point of carapace.*

Inapplicable for taxa lacking a carapace (Character 24). There is a lot of variety of this character amongst "carapace-bearing arthropods", with isoxyids typically possessing a shallow carapace posterior with the tallest point occurring in the anterior half of the domicilium, whist protocaridids are more rounded, with the tallest point occurring towards the middle, and fuxianhuids towards the posterior of the carapace.

2. *Height to length ratio of carapace domiciluium.*

Inapplicable for taxa lacking a carapace (Character 24). This character serves to distinguish the carapaces of most "carapace-bearing arthropods", in which the carapace is typically longer than wide, from fuxianhuids, in which the carapace is wider than long.

3. *Length of antero-dorsal carapace spines.*

Inapplicable for taxa lacking antero-dorsal carapace spines (Character 29). This character specifically refers to species of *Isoxys*. Both *I. volucris*, and *I. curvirostratus* possess an elongate antero-dorsal spine, whilst that of *I. acutangulus* and *I. auritus* is much shorter.

4. *Length of postero-dorsal carapace spines*.

Inapplicable for taxa lacking postero-dorsal carapace spines (Character 29). This character specifically refers to species of *Isoxys*.

5. *Slope of posterior carapace margin*.

Inapplicable for taxa lacking a carapace (Character 24). This character serves to distinguish *Isoxys* from other species of "carapace-bearing arthropods". *Isoxys* is unique in possessing a deeply sloped posterior carapace margin.

Meristic characters

Meristic characters were analysed as continuous characters. This differs from previous analyses that have treated them as discrete, thereby creating arbitrary bins and reducing character linkage and hindering trait determination.

Trunk

6. *Number of trunk segments*.

This character could not be determined for many taxa bearing a carapace, as this feature frequently covers an anterior series of poorly sclerotized trunk segments (e.g. *Nereocaris, Loricicaris*). Likewise, this character was not coded for the trilobite *Olenoides serratus*, as the exact number of segments in the pygidium could not be determined.

7. *Number of prothoracic segments*.

This character is inapplicable for taxa lacking a prothorax (Character 42). The fuxianhuidids, namely *Guangweicaris spinatus*, *Fuxianhuia protensa*, and *F. xiaoshibaensis*, possess three prothoracic segments, whilst the chengjiangocaridids, *Alacaris mirabilis*, *Chengjiangocaris longiformis*, and *C. kunmingensis*, possess five, and *Shankoia zhenghei* possesses six. This character could not be adequately determined for *Liangwangshania biloba* as there is little variation between the morphology of the posterior prothoracic segments and the anterior post-prothoracic segments.

8. *Number of post-prothoracic thorax segments*.

This character is inapplicable for taxa lacking a prothorax (Character 42). Unfortunately, the extent of the thorax could not be determined in a number of fuxinhuids as the position of the appendage, which would serve to delineate the thorax in taxa without a posteriorly differentiated abdomen, could also not be determined. *Guangweicaris spinatus* possesses a short, five segmented, post-prothoracic thorax, whilst the two species of *Fuxianhuia* both possess 17.

9. *Number of abdominal segments*.

This character is inapplicable for taxa lacking a distinct abdomen delineated by either a lack of appendages, or a notable change in dimension from the anterior (thoracic) trunk segments.

Appendicular (cephalic)

10. *Number of podomeres in pre-antennular (protocerebral) appendages*.

This character is inapplicable for taxa lacking an arthropodized protocerebral appendage with distinct podomeres (Character 50).

11. *Number of post-protocerebral cephalic appendage pairs in cephalic region*.

This character is inapplicable for taxa lacking a distinct sclerotized cephalic covering, and could not be determined in most "carapace-bearing arthropods" due to uncertainty regarding the position of the cephalon-trunk boundary. In fuxianhuids this can be determined based on the position of the prothorax relative to the anterior appendages.

12. *Number of podomeres in differentiated tritocerebral appendage*.

This character is inapplicable for taxa lacking a pair of differentiated tritocerebral appendage (Character 61). All fuxianhuids for which a differentiated tritocerebral appendage is known possess three segments in each appendage, whilst megacheirans possess either five or six, and the protocaridids, *Branchiocaris pretiosa* and *Tokumnia katalepis* both possess eight.

13. *Number of spine-bearing distal podomeres on tritocerebral appendage.*

This character is inapplicable for taxa lacking spinose projections on a differentiated tritocerebral appendage (Character 61).

Appendicular (general)

14. *Number of exite segments*.

This character is inapplicable for taxa lacking exites (Character 65). This character serves to distinguish advanced megacheirans, specifically *Yohoia tenuis* and *Leanchoilia superlata*, and the trilobite *Olenoides serratus*, which possess an exite composed of two segments, from the other megacheirans, and stem-lineage euarthropods, including the dinocaridids, and "carapace-bearing arthropods", which possess just a singular segment.

15. *Number of trunk endopod segments (podomeres).*

Appendicular (lateral processes)

16. *Number of lateral process pairs.*

Discrete characters

Cephalic (including external ocular features)

17. *Anterior (ocular) sclerite: (0) absent, (1) present*.

18. *Anterior margin of anterior sclerite tapered: (0) absent, (1) present*.

19. *Anterior sclerite flanked by lateral plates: (0) absent, (1) present*.

20. *Lateral eyes: (0) absent, (1) present*.

21. *Lateral eyes stalked: (0) absent, (1) present*.

22. *Single medial eye: (0) absent, (1) present*.
23. *Sclerotized cephalic covering: (0) absent, (1) present*.

Cephalic (carapace)

24. *Free posterolateral extensions of sclerotized cephalic covering: (0) absent, (t) present*.
25. *Antero-ventral and postero-dorsal margins of carapace parallel: (0) absent, (1) present*.
26. *Carapace reticulate: (0) absent, (1) present*.
27. *Reticulation type: (0) small mesh, (1) large, hexagonal, mesh*.
28. *Anterior extension of carapace: (0) absent, (1) present*.
29. *Anterodorsal spine: (0) absent, (1) present*.
30. *Anteroventral hook-like processes: (0) absent, (1) present*.
31. *Posterodorsal keel: (0) absent, (1) present*.
32. *Carapace divided medial by suture or hinge: (0) absent, (1) present*.
33. *Posteromedial suture on carapace: (0) absent, (1) present*.
34. *Posterodorsal spine: (0) absent, (1) present*.
35. *Lateral margins of carapace contiguous with lateral pleural trunk margins: (0) absent, (1) present.*

Trunk

36. *Sclerotized trunk: (0) absent, (1) present*.
37. *Paired dorsal nodes: (0) absent, (1) present*.
38. *Dorsal band of blade-like setae: (0) absent, (1) present*.
39. *Pleural extension oftergites: (0) absent, (1) present*.
40. *Posterolateral margins of pleurae extended into spinose projections: (0) absent, (1) present.*
41. *Raised axial region: (0) absent, (1) present*.
42. *Anterior trunk segments greatly reduced forming a prothorax: (0) absent, (1) present*.
43. *Abdomen differentiated as limb-free segments: (0) absent, (1) present*.
44. *Abdomen differentiated as posteriorly-restricted segments: (0) absent, (1) present*.
45. *Posterior trunk segments with spinose posterior rim: (0) absent, (1) present*.
46. *Penultimate trunk segment elongate: (0) absent, (1) present*.

Telson

47. *Telson: (0) absent, (1) present*.

Appendicular (pre-antennular, protocerebral)

48. *Protocerebral appendages: (0) absent, (1) present*.
49. *Orientation of protocerebral appendages: (0) lateral, (1) ventral*.
50. *Sclerotization of protocerebral appendages: (0) absent, (1) present*.
51. *Fusion of protocerebral appendages: (0) absent, (1) present*.
52. *Hypostome with lateral slits: (0) absent, (1) present*.
53. *Protocerebral appendages spinose: (0) absent, (1) present*.
54. *Dorsal spine row: (0) absent, (1) present*.
55. *Ventral spine row: (0) absent, (1) present*.
56. *Relative orientation of dorsal spine row to podomere: (0) perpendicular, (1) lateral (chelate)*.
57. *Elongate ventral basal spine: (0) absent, (1) present*.
58. *Secondary (auxillary) spines on ventral spine row: (0) absent, (1) present*.
59. *Flexure of terminal protocerebralpodomere: (0) ventral, (1) dorsal*.

Appendicular (antennular, deutocerebral)

60. *Deutocerebral appendage differentiated from posterior appendages: (0) absent, (1) present*.

Appendicular (First-post-antennular, tritocerebral)

61. *Tritocerebral appendage differentiated from posterior appendages: (0) absent, (1) present*.
62. *Basal podomere bearing endites: (0) absent, (1) present*.
63. *Appendages geniculate with distinct peduncle: (0) absent, (1) present*.
64. *Chelate (or subchelae) distal podomeres: (0) absent, (1) present*.

Appendicular (post-tritocerebral)

65. *Exites: (0) absent, (1) present*.
66. *Longitudinal wrinkling on exites: (0) absent, (1) present*.
67. *Exite fringed with setae: (0) absent, (1) present*.

68. *Exite and endopod derived from the same parent podomere (biramy): (0) absent, (1) present*.
69. *Trunk endopods: (0) absent, (1) present*.
70. *Endopod shape: (0) leg-like, (1) flap-like*.
71. *Sclerotization and arthropodization of trunk endopods: (0) absent, (1) present*.
72. *Endites on endopod: (0) absent, (1) present*.
73. *Endites on basal endopod segment: (0) absent, (1) present*.
74. *Endopod with terminal claws: (0) absent, (1) present*.

Appendicular (lateral processes)

75. *Posterior tagmata with elongate lateral processes: (0) absent, (1) present*.
76. *Lateral process pairs fused into a single element retaining evidence of original segmentation: (0) absent, (1) present*.
77. *Shape of lateral processes: (0) bulbous (unsclerotized) flaps, (1) cerci, (2) sub-triangular, (3) paddle-like*.
78. *Lateral telson processes recurved: (0) absent, (1) present*.
79. *Lateral telson processes spinose: (0) absent, (1) present*.

Digestive

80. *Orientation of mouth: (0) anterior, (1) ventral, (2) posterior*. [ADDITIVE]
81. *Circumoral structures: (0) absent, (1) present*.
82. *Nature of circumoral structures: (0) papillae, (1) sclerotized plates*.
83. *Lateral gut glands: (0) absent, (1) present*.

Supplementary References

1. Yang, J., *et al.* A superarmored lobopodian from the Cambrian of China and early disparity in the evolution of Onychophora. *Proc. Natl. Acad. Sci., U.S.A.* **112**, 8678–8683 (2015).

2. Yang, J., Ortega-Hernández, J., Butterfield, N. J. & Zhang, X.-G. Specialized appendages in fuxianhuiids and the head organization of early euarthropods. *Nature* **494**, 468–471 (2013).

3. Li, S.-J., Kang, C.-L. & Zhang, X.-G. Sedimentary environment and trilobites of Lower Cambrian Yuxiansi Formation in Leshan District. *Bull. Chengdu Inst. Geol. Min. Resour., Chinese Acad. Geol. Sci.* **12**, 37–56 (1990) [in Chinese].

4. Ortega-Hernández, J. Making sense of 'lower' and 'upper' stem-group Euarthropoda, with comments on the strict use of the name Arthropoda von Siebold, 1848. *Biol. Rev.* **91**, 255–273 (2016).5. Bousfield, E. I. A contribution to the natural classification of Lower and Middle Cambrian arthropods: food gathering and feeding mechanisms. *Amphipacifica* **2**, 3–34 (1995).

6. Waloszek, D., Chen, J.-Y., Maas, A. & Wang, X.-Q. Early Cambrian arthropods—new insights into arthropod head and structural evolution. *Arthropod Struct. Dev.* **34**, 189–205 (2005).

7. Chen, A.-L. A new *Fuxianhuia*-like arthropod of the early Cambrian Chengjiang fauna in Yunnan. *Yunnan Geol.* **24**, 108–113 (2005).

8. Hou, X.-G. & Bergström, J. Arthropods of the Lower Cambrian Chengjiang fauna, southwest China. *Fossils Strata* **45**, 1–116 (1997).

9. Luo, H.-L., Fu, X., Hu, S.-X., You, T., Pang, J. & Liu, Q. A new arthropod *Guangweicaris* gen. nov. (Luo, Fu *et* Hu) from the Early Cambrian Guanshan fauna, Kunming, China. *Acta Geol. Sin.* **81**, 1–7 (2007).

10. Hou, X.-G. Three new large arthropods from Lower Cambrian, Chengjiang, eastern Yunnan. *Acta. Palaeontol. Sin.* **26**, 272–285 (1987).

11. Bergström, J., Hou, X.-G., Zhang, X.-G., Liu, Y. & Clausen, S. A new view of the Cambrian arthropod *Fuxianhuia*. *GFF* **130**, 189–201 (2008).

12. Yang, J., Hou, X.-G. & Dong, W. Restudy of *Guangweicaris* Luo, Fu et Hu, 2007, from the Lower Cambrian Canglangpu Formation in Kunming area. *Acta Palaeontol. Sin.* **47**, 115–122 (2008).

13. Hou, X.-G. & Bergström, J. The arthropods of the Lower Cambrian Chengjiang fauna, with relationships and evolutionary significance. in *The Early Evolution of Metzoan and the Significance of Problematic Taxa* (eds Simonetta, A. M. & Conway Morris, S.) 179–187 (Cambridge Univ. Press, Cambridge 1991).